

1 **Fast Evaluation of Viral Emerging Risks (FEVER): A computational tool for**  
2 **biosurveillance, diagnostics, and mutation typing of emerging viral pathogens**

3  
4 Zachary R. Stromberg,<sup>a</sup> James Theiler,<sup>b</sup> Brian T. Foley,<sup>c</sup> Adán Myers y Gutiérrez,<sup>d</sup> Attelia  
5 Hollander,<sup>d</sup> Samantha J. Courtney,<sup>a</sup> Jason Gans,<sup>d</sup> Alina Deshpande,<sup>d</sup> Ebany J. Martinez-Finley,<sup>e</sup>  
6 Jason Mitchell,<sup>e</sup> Harshini Mukundan,<sup>a</sup> Karina Yusim,<sup>c</sup> Jessica Z. Kubicek-Sutherland<sup>a,#</sup>

7  
8 <sup>a</sup> Physical Chemistry and Applied Spectroscopy, Los Alamos National Laboratory, Los Alamos,  
9 New Mexico, United States

10 <sup>b</sup> Space Data Science and Systems, Los Alamos National Laboratory, Los Alamos, New Mexico,  
11 United States

12 <sup>c</sup> Theoretical Biology and Biophysics, Los Alamos National Laboratory, Los Alamos, New  
13 Mexico, United States

14 <sup>d</sup> Biosecurity and Public Health, Los Alamos National Laboratory, Los Alamos, New Mexico,  
15 United States

16 <sup>e</sup> Presbyterian Healthcare Services, Albuquerque, New Mexico, United States

17

18 **Short Title:** FEVER tool for detecting emerging viral pathogens

19 # Corresponding author: [jzk@lanl.gov](mailto:jzk@lanl.gov)

## 20 ABSTRACT

21           Viral pathogen can rapidly evolve, adapt to novel hosts and evade human immunity. The  
22 early detection of emerging viral pathogens through biosurveillance coupled with rapid and  
23 accurate diagnostics are required to mitigate global pandemics. However, RNA viruses can mutate  
24 rapidly, hampering biosurveillance and diagnostic efforts. Here, we present a novel computational  
25 approach called FEVER (Fast Evaluation of Viral Emerging Risks) to design assays that  
26 simultaneously accomplish: 1) broad-coverage biosurveillance of an entire class of viruses, 2)  
27 accurate diagnosis of an outbreak strain, and 3) mutation typing to detect variants of public health  
28 importance. We demonstrate the application of FEVER to generate assays to simultaneously 1)  
29 detect sarbecoviruses for biosurveillance; 2) diagnose infections specifically caused by severe  
30 acute respiratory syndrome coronavirus 2 (SARS-CoV-2); and 3) perform rapid mutation typing  
31 of the D614G SARS-CoV-2 spike variant associated with increased pathogen transmissibility.  
32 These FEVER assays had a high *in silico* recall (predicted positive) up to 99.7% of 525,708 SARS-  
33 CoV-2 sequences analyzed and displayed sensitivities and specificities as high as 92.4% and 100%  
34 respectively when validated in 100 clinical samples. The D614G SARS-CoV-2 spike mutation  
35 PCR test was able to identify the single nucleotide identity at position 23,403 in the viral genome  
36 of 96.6% SARS-CoV-2 positive samples without the need for sequencing. This study demonstrates  
37 the utility of FEVER to design assays for biosurveillance, diagnostics, and mutation typing to  
38 rapidly detect, track, and mitigate future outbreaks and pandemics caused by emerging viruses.

## 39 INTRODUCTION

40 In the last decade, several RNA viruses have emerged from animal reservoirs to threaten  
41 global public health (1). These viruses include influenza A in 2009 (2), Ebola in 2013 (3),  
42 Chikungunya in 2014 (4), Zika in 2015 (5), and severe acute respiratory syndrome coronavirus 2  
43 (SARS-CoV-2) most recently in 2019 (6, 7). Outbreaks and pandemics often occur when a  
44 zoonotic viral strain evolves and escapes human immunity (8, 9). The early detection of these  
45 pathogens is required to minimize outbreaks and prevent pandemics by guiding early interventions  
46 (10). However, RNA viruses mutate rapidly, so biosurveillance tools must be able to detect groups  
47 of viral pathogens with diverse genome sequences and emerging variants, often requiring time-  
48 consuming and expensive procedures performed by trained personnel that are not easily accessible  
49 in all regions of the world (11, 12). Once spillover occurs and a viral isolate enters human  
50 circulation, a rapid and accurate diagnostic test is required to circumvent its spread (13-16).  
51 However, development of accurate diagnostics at the onset of an outbreak can be challenging due  
52 to limited data availability depending on the location of the outbreak, and the process for validation  
53 and implementation of a new test can also be time-consuming (17). Having a broadly applicable  
54 computational approach to assay design that can accommodate pathogen emergence and variant  
55 evolution would help alleviate some of these challenges.

56 Coronaviruses are positive-sense, single-stranded RNA viruses and a leading cause of the  
57 common cold (18). However, several recent coronavirus outbreaks, including SARS-CoV in 2002-  
58 2003, and Middle East respiratory syndrome coronavirus (MERS-CoV) in 2012, were associated  
59 with significant morbidity and mortality (8, 19, 20). In December 2019, SARS-CoV-2 emerged in  
60 humans and spread rapidly, resulting in the COVID-19 (coronavirus disease 2019) global  
61 pandemic (21-23). SARS-CoV-2, along with SARS-CoV and SARS-like viruses, belong to the

62 subgenus *Sarbecovirus* (24). Effective diagnostic and biosurveillance assays are critical to control  
63 the spread of SARS-CoV-2 and prevent future *Sarbecovirus* pandemics.

64 Real-time reverse transcription PCR (RT-PCR) is considered the gold standard for  
65 COVID-19 diagnostics (25) with assays developed by the United States Centers for Disease  
66 Control and Prevention (U.S. CDC) (26), China CDC (27), Hong Kong University (28), and  
67 Charité Institute of Virology (29), along with commercial products (30). Traditionally, RT-PCR  
68 probe and primer design involved selecting a target from a specific gene, often a virulence factor  
69 (31). In contrast, modern probe and primer design involves multiple sequence alignments and  
70 algorithms to determine conserved signatures for detection (32-34). However, if assays are not  
71 updated periodically to account for variants, genome mutations can emerge at the primer or probe  
72 binding site and limit assay utility (35, 36). The U.S. CDC initially designed a pan-*Sarbecovirus*  
73 assay targeting the nucleocapsid gene (2019-nCoV\_N3) with broad coverage, however it  
74 eliminated this assay from its diagnostic panel to simplify the testing process (37) and because of  
75 cross-reactivity (38) and false-negative results on clinical samples (39). Also, mutations at either  
76 a primer or probe binding site (not specified because of proprietary components) yielded false-  
77 negative results for the Roche cobas envelope gene pan-*Sarbecovirus* assay (36). Finally,  
78 mutations have made SARS-CoV-2 more transmissible (40, 41) and potentially more resistant to  
79 immunity induced by vaccination (42). The current practice of independently introducing  
80 biosurveillance efforts, targeted diagnostics and mutation tracking has hampered our ability to  
81 adapt and respond to the dynamic challenges presented by the COVID-19 pandemic. The  
82 development of a synchronous approach to integrate these data streams can help mitigate the  
83 challenges posed by emerging viral pathogens and support rapid decision making to help combat  
84 future outbreaks and pandemics.

85           There is a critical need for tools that can be used in biosurveillance and diagnostic  
86 applications to respond rapidly to emerging pathogens and mitigate their global impact (43). To  
87 this end, we have developed FEVER (Fast Evaluation of Viral Emerging Risks), a computational  
88 approach that can generate both high-coverage or strain-specific diagnostic assays so that the same  
89 detection platform can be used for both broad-based biosurveillance and targeted diagnostic  
90 applications. Here, we demonstrate the applicability of FEVER for simultaneous biosurveillance  
91 of pan-*Sarbecoviruses* and targeted diagnosis of SARS-CoV-2 in a cohort of 100 human patients.  
92 We also demonstrate mutation typing of the D614G SARS-CoV-2 spike variant using this  
93 approach as an example of a rapid method for tailored surveillance of pathogen evolution and  
94 emergence.

## 95 MATERIALS AND METHODS

96 **Ethics.** This study was designed in alignment with DOE, NIH, and universal HIPAA  
 97 guidelines. The protocol was reviewed and approved by the Institutional Review Board of the Los  
 98 Alamos National Laboratory (LANL#000473), per DOE guidelines and policies, and by the  
 99 Presbyterian Institutional Review Board (PHS IRB#1608836).

100  
 101 **FEVER surveillance and diagnostic probe and primer design.** For the surveillance and  
 102 diagnostics FEVER assays, four sets of primers and probes were generated (Table 1). Two sets of  
 103 primers and probes were developed for universal detection of all sarbecoviruses, with one targeting  
 104 the 5' untranslated region (UTR) termed FEVER\_5'UTR and another targeting the envelope gene  
 105 termed FEVER\_Env. Another two sets of primers and probes were developed for specific  
 106 detection of SARS-CoV-2, with one targeting the ORF1ab region termed FEVER\_ORF1ab and  
 107 one targeting the spike gene called FEVER\_Spike. After the FEVER probes were designed,  
 108 primers flanking the probes were created by the PrimerDesign-M tool (44, 45) using an alignment  
 109 of SARS-CoV-2 sequences.

**Table 1. FEVER Assays for COVID-19**

Gene target	Primer or probe name	Sequence 5' to 3'	Final conc. (nM)
<b>Pan-Sarbecovirus detection</b>			
5'UTR	FEVER_5'UTR_F	CTGCTTACGGTTYCGTCCGIGTTGC	500
	FEVER_5'UTR_R	ACTGAGTTGGACGTGTGTTTTCTC	500
	FEVER_5'UTR_P	FAM-CTCTCCATC/ZEN/TTACCTTCGGTCACACCCGG-IABkFQ	250
Envelope	FEVER_Env_F	CCGACGACGACTACTAGCG	500
	FEVER_Env_R	GTTTAGACCAGAAGATCAGGAAC	500
	FEVER_Env_P	FAM-CGCACACAA/ZEN/TCGAAGCGCAGTAAGGATGGCT-IABkFQ	250
<b>Specific SARS-CoV-2 detection</b>			
ORF1ab	FEVER_ORF1ab_F	ATGAAGTATTTTGTGAAAATAGG	500
	FEVER_ORF1ab_R	CAGCTAGACACCTAGTCATG	500
	FEVER_ORF1ab_P	FAM-TCTGAAGCA/ZEN/GTGGAAAAGCATGTGGCACGT-IABkFQ	250
Spike	FEVER_Spike_F	TCCCTCAGGGTTTTTCGGCTTTAG	500
	FEVER_Spike_R	GTTTCTGAGAGAGGGTCAAGTGCAC	500
	FEVER_Spike_P	FAM-TGCAGCACCC/ZEN/AGCTGTCCAACCTGAAGAAGAA-IABkFQ	250
<b>Mutation typing</b>			
Spike	23403_F	CCAGGAACAAATACTTCTAACCAGGTT	900
	23403_R	GCATGAATAGCAACAGGGACTTCT	900
	23403_P1(Wuhan)	VIC-TGTTCTTTATCAGGA <sup>T</sup> TGTTAAC-NFQ	200

---

Bold/underlined nucleotide indicates the position at which the SNP is detected.

110

111 ***Sequence data.*** As of March 10, 2020 the Global Initiative on Sharing All Influenza Data  
112 (GISAID) database (<https://www.epicov.org> or <https://www.gisaid.org/>) had acquired 338  
113 complete, or near-complete, high-quality SARS-CoV-2 genome sequences. After aligning the  
114 sequences and eliminating all but one of each set of sequences which were 100% identical to each  
115 other to reduce redundancy, our data set consisted of 19 unique sequences of SARS-CoV-2. We  
116 also collected all coronaviruses from GenBank that were in the “Sarbecovirus clade” of the beta  
117 coronaviruses, using BLAST searches rather than GenBank taxonomy because many  
118 sarbecoviruses were listed as “unclassified coronavirus” in the taxonomy table. Again, we reduced  
119 redundancy by eliminating identical sequences (primarily many dozens of SARS sequences from  
120 the 2003-2004 outbreak), and retained a set of 67 genome sequences. It was these 86 *Sarbecovirus*  
121 genomes that were used to design our assays.

122 ***FEVER algorithm.*** The FEVER algorithm does not require sequence alignments prior to  
123 probe design. Instead, our probe design goal was to produce a short nucleotide sequence (called a  
124 “*k*-mer”, *e.g.*, a short DNA sequence, *k* base pairs long) that binds to SARS-CoV-2 without binding  
125 to background material that may be present in a sample that is being tested. Specific desirable  
126 properties of the probe included maintaining a high GC-content and reducing the hairpin  
127 propensity (*i.e.*, the tendency of the probe string to fold over on itself) by ensuring that any self-  
128 complementary pairs of sub-strings in the probe are sufficiently short. The mathematical  
129 formalization of the problem was expressed in terms of a constrained optimization, with minimum  
130 GC-content and the maximum length of self-complementary sub-strings taken as constraints while  
131 maximizing coverage. A probe is said to “cover” a SARS-CoV-2 sequence if the probe’s *k*-mer  
132 appears as a sub-sequence of that sequence. Thus, coverage is defined as the number of sequences

133 in the database covered by the probe. "Exact" coverage corresponds to an exact match of probe  
134 and sub-sequence. Hamming distance between two strings is defined as the number of characters  
135 that would have to be changed in one string to agree with the other string. Given a database of  
136 SARS-CoV-2 sequences, the single probe design problem is to find a string of length  $k$ , subject to  
137 the constraints of GC-content and hairpin aversion, that covers as many SARS-CoV-2 sequences  
138 as possible. For the multi-probe design problem, we seek  $n$  probes instead of just one, and a  $n$ -  
139 probe design is said to cover a SARS-CoV-2 sequence if any one of the probes covers it. The  
140 selection of  $k=31$  was used because of practical considerations for molecular beacon synthesis  
141 allowing for a 12 bp stem region (6 bp on each side of the  $k$ -mer). Also,  $k=31$  was long enough to  
142 bind to target sequences in the SARS-CoV-2 database without accidentally covering potential  
143 background sequences.

144 Our FEVER algorithm works by extracting all  $k$ -mers from each of the sequences in the  
145 database and then restricting consideration to those that exhibit a minimal GC-content and hairpin  
146 aversion. For every one of these  $k$ -mers, we counted how many viral sequences were covered,  
147 being careful not to count a sequence twice even if the  $k$ -mer appears twice in it. Finally, we  
148 selected the  $k$ -mer with the largest count. To ensure that our probes were not susceptible to viral  
149 mutation, a multi-probe design approach was applied. The first probe was designed using a naïve  
150 approach by producing the optimal probe with highest coverage of the queried sequence  
151 database. The next probe is designed by eliminating the viral sequences covered by the first probe  
152 and using this truncated database to find the single probe that best covers the remaining viral  
153 sequences. This process is repeated until 100% of the database is covered. For both pan-  
154 *Sarbecovirus* sequences and SARS-CoV-2 sequences it only took 2 probes to obtain 100%  
155 coverage of the sequence database at the time of design.



156            **Data availability.** All code written in support of this publication is publicly available at  
157 <https://github.com/jt-lanl/fever-probes>.

158  
159            **FEVER mutation typing probe and primer design.** A variant carrying the amino acid  
160 change D614G spike mutation became globally dominant, and the G614 variant has been  
161 demonstrated to have a fitness advantage associated with higher viral loads (40). A custom  
162 TaqMan SNP Genotyping Assay was designed (Thermo Fisher, 4332075) to detect this single  
163 nucleotide polymorphism (SNP) in SARS-CoV-2 using Thermo Fisher Scientific’s Custom Assay  
164 Design Tool. Probe and primer sequences are presented in Table 1.

165  
166            **Analysis of primer and probe coverage.** The FEVER biosurveillance and diagnostics  
167 assays were computationally characterized using two complementary methods. First, the  
168 frequency of SARS-CoV-2 variants in the amplified region of the FEVER and U.S. CDC assays  
169 were assessed visually using the Variant Visualizer, which is under development and will be  
170 available at <https://cov.lanl.gov>. Second, we used an *in silico* validation tool (46) to assess the  
171 inclusivity of the FEVER assays compared with the U.S. CDC N1 and N2 assays (26). Each assay  
172 (forward primer, reverse primer and TaqMan probe) was evaluated against each SARS-CoV-2  
173 sequence from GISAID (47) public database that was greater than 29 kb ( $n = 525,708$ ) to ensure  
174 only complete genomes were assessed. The GISAID sequence data used in this analysis was  
175 accessed on February 15, 2021. Results are presented in Table 2. For this analysis, a false-negative  
176 was assigned if one or more assay oligonucleotides satisfied any of the following conditions: (i)  
177 three or more mismatches to a target sequence, (ii) a predicted melting temperature less than 40°C  
178 between the oligonucleotide and a target sequence, or (iii) when primer/target mismatches

179 occurred in either of the last two 3' bases of a primer associated with an expected increase of 2 or  
 180 more in the cycle threshold ( $C_T$ ) value (as defined previously (48)). True-positives were assigned  
 181 for any assay/target sequence pairing that did *not* result in a false negative. Results are also reported  
 182 as the number of genome sequences that contained perfect matches, single mismatches, two  
 183 mismatches, or three or more mismatches for a given assay.

**Table 2. *In silico* inclusivity test against SARS-CoV-2 sequences.**

Assay	Recall (%) <sup>a</sup>	No. sequences with perfect match	No. sequences with 1 mismatch	No. sequences with 2 mismatches	No. sequences that failed <sup>b</sup>
FEVER_5'UTR	96.39	413,603	91,763	1,361	18,981
FEVER_Env	98.63	511,976	6,164	343	7,225
FEVER_ORF1ab	99.72	490,388	33,723	143	1,454
FEVER_Spike	90.51	360,033	115,321	481	49,873
U.S. CDC N1	98.95	506,092	11,454	2,633	5,529
U.S. CDC N2	99.17	507,298	13,901	156	4,353

Oligonucleotides from each assay were assessed against 525,708 sequences of SARS-CoV-2 obtained from GISAID on February 15, 2021.

<sup>a</sup>Recall = true-positive (sum of the perfect match, single mismatch, and double mismatch) / (true-positive + false negative).

<sup>b</sup>Failure represents SARS-CoV-2 sequences that were not detected (false-negative).

184

185 **Patient sample collection.** From November 2020 to December 2020, 100 nasopharyngeal  
 186 (NP) swabs were collected from individuals suspected of having COVID-19 disease or otherwise  
 187 randomly tested in the U.S. state of New Mexico. NP swabs were collected using existing U.S.  
 188 CDC guidelines, labeled with a de-identified bar code, and stored under refrigerated conditions  
 189 until batch shipping (within 24 hours of sample collection). Specimens were packed and shipped  
 190 according to U.S. Department of Transportation regulations regarding the shipment of biological  
 191 substances.

192

193 **RNA extraction.** For spiked samples, RNA extraction was performed using the QIAamp  
 194 Viral RNA Mini Kit (Qiagen). For the NP swab samples, RNA was extracted using the MagMAX  
 195 Viral/Pathogen Nucleic Acid Isolation Kit (Thermo Fisher) and a KingFisher. For both kits, a 200

196  $\mu\text{L}$  portion of each sample was used for extraction following the manufacturer's instructions with  
197 a 50  $\mu\text{L}$  elution, and 5  $\mu\text{L}$  of the eluted template was used in RT-PCR.

198

199 **RT-PCR protocol.** Samples were tested using our FEVER and U.S. CDC 2019-novel  
200 coronavirus (2019-nCoV) RT-PCR diagnostic panel (termed U.S. CDC assays) (26). For the U.S.  
201 CDC N1 (2019-nCoV\_N1) and N2 (2019-nCoV\_N2) assays, each 20  $\mu\text{L}$  reaction consisted of 8.5  
202  $\mu\text{L}$  of water, 1.5  $\mu\text{L}$  of combined primer and probe mix (IDT, 500 nM primer and 125 nM probe,  
203 final concentrations), 5  $\mu\text{L}$  of TaqPath 1-step RT-qPCR master mix (Thermo Fisher), and 5  $\mu\text{L}$  of  
204 the template. For the FEVER assays (FEVER\_5'UTR, FEVER\_Env, FEVER\_ORF1ab, and  
205 FEVER\_Spike), each 20  $\mu\text{L}$  reaction consisted of 8  $\mu\text{L}$  of water, 2  $\mu\text{L}$  of combined primer and  
206 probe mix (IDT, 500 nM primer and 250 nM probe, final concentrations), 5  $\mu\text{L}$  of TaqPath 1-step  
207 RT-qPCR master mix, and 5  $\mu\text{L}$  of the template. The thermocycling conditions were the same for  
208 all assays. Thermocycling conditions using an ABI StepOnePlus or 7500 Fast Dx were 25°C for 2  
209 min, 50°C for 15 min, 95°C for 2 min, followed by 45 cycles of 95°C for 3 s and 55°C for 30 s.  
210 For RT-PCR assays, samples were considered positive when the  $C_T$  value  $\leq 40$ . Patient clinical  
211 samples were considered positive for SARS-CoV-2 when the two U.S. CDC assays N1 and N2  
212 both had a  $C_T$  value  $\leq 40$ , and negative when both targets had a  $C_T$  value  $> 40$  according to CDC  
213 guidelines (37). If only one N1 or N2 result was positive, the result was considered inconclusive  
214 and the sample was re-run. If the re-test results were also inconclusive, the final result was reported  
215 as inconclusive.

216

217 **Analytical specificity of RT-PCR.** The analytical specificities of the FEVER and U.S.  
218 CDC assays were evaluated using genomic RNA from various viruses obtained from BEI

219 resources. We tested 5  $\mu$ L of undiluted genomic RNA preparation from SARS-CoV Urbani (NR-  
220 52346), avian coronavirus Massachusetts (NR-49096), alphacoronavirus Purdue P115 (NR-  
221 48571), porcine respiratory coronavirus ISU-1 (NR-48572), two influenza A viruses (NR-20080  
222 and NR-20081), and two influenza B viruses (NR-45848 and NR-45849). RNA from heat-  
223 inactivated SARS-CoV-2 isolate USA-WA1/2020 (BEI Resources, NR-52347) was a positive  
224 assay control, and water was a negative assay control.

225

226 **Analytical sensitivity.** The analytical sensitivity of each assay was determined by spiking  
227 inactivated SARS-CoV-2 USA-WA1/2020 strain (BEI resources, NR-52286) at  $10^4$  copies/ $\mu$ L,  
228 and 10-fold serial dilutions were performed in an NP swab matrix. NP swabs from a single human  
229 donor (Lee Biosolutions, #991-31-NC-COVID-N) were suspended in 0.45% saline and confirmed  
230 SARS-CoV-2 negative by the supplier. Each concentration was tested using three biological  
231 replicates.

232

233 **Assessment of NP swab samples.** The 100 NP swab samples were transported to the  
234 laboratory for RNA extraction and testing. After RNA extraction, samples were stored at  $-80^\circ\text{C}$ .  
235 Samples were tested by our FEVER and U.S. CDC assays for SARS-CoV-2. For the U.S. CDC  
236 assays, the 2019-Ncov plasmid (IDT) containing the nucleocapsid gene was used as a positive  
237 control, and water was used as a negative control. For the FEVER assays, RNA from heat-  
238 inactivated SARS-CoV-2, isolate USA-WA1/2020 (BEI Resources, NR-52347) was used as a  
239 positive control, and water was used as a negative control. The RNase P assay described by the  
240 U.S. CDC assays (26) was used as an extraction control for each sample.

241

242           **Mutation typing of SARS-CoV-2 by PCR.** Extracted RNA (10  $\mu$ L) from SARS-CoV-2  
243 positive patient samples was reverse transcribed in a 20  $\mu$ L reaction using the High Capacity cDNA  
244 Reverse Transcription Kit (Thermo Fisher, 4368814) according to the manufacturer's instructions.  
245 Each 20  $\mu$ L SNP genotyping PCR reaction consisted of 5  $\mu$ L of cDNA as the template, 4.5  $\mu$ L of  
246 water, 0.5  $\mu$ L of 40 $\times$  SNP genotyping mix (900 nM primer and 200 nM probe final concentrations),  
247 and 10  $\mu$ L of 2 $\times$  TaqMan Genotyping Master Mix (Thermo Fisher, 4371353). Amplification was  
248 performed using an ABI StepOnePlus RT-PCR machine under the following conditions: 10 min  
249 at 95 $^{\circ}$ C and 45 cycles of 15 s at 95 $^{\circ}$ C and 60 s at 60 $^{\circ}$ C in a 96-well plate. The PCR  $C_T$  values  
250 corresponding with the wild type (VIC) and mutant (FAM) forms were compared, and the lower  
251 value ( $\leq 45$ ) of the two was determined to be the SNP sequence. Samples were considered  
252 undetermined when both reactions had a  $C_T$  value  $>45$ . Control RNA from Heat-Inactivated  
253 SARS-CoV-2, isolate USA-WA1/2020 (BEI Resources, NR-52347) was used as a positive  
254 control, diluted to  $10^4$  copies/ $\mu$ L, and run with each batch of cDNA synthesis and PCR. Isolate  
255 USA-WA1/2020 contains the wild-type spike sequence, and all results with this control showed  
256 that the wild-type  $C_T$  was lower than the mutant  $C_T$  value (data not shown).

257           A total of 17 NP swab samples had sufficient sample volume to be used in sequencing to  
258 confirm the D614G mutation. The spike gene was amplified using the 23403F\_seq and  
259 23403R\_seq primers (5'- TGAACTTCTACATGCACCAGC -3' and 5'-  
260 AAACAGCCTGCACGTGTTTG -3', respectively). Each 25  $\mu$ L reaction consisted of 5  $\mu$ L of  
261 cDNA as the template, 11.75  $\mu$ L of water, 5  $\mu$ L of 5X Q5 reaction buffer (New England BioLabs),  
262 0.5  $\mu$ L of 10 mM dNTPs, 1.25  $\mu$ L of each primer (0.5  $\mu$ M final concentration), and 0.25  $\mu$ L of Q5  
263 hot start high-fidelity DNA polymerase (New England BioLabs). PCR was performed on a  
264 thermocycler as follows: 30 s at 95 $^{\circ}$ C and 35 cycles of 10 s at 98 $^{\circ}$ C, 30 s at 65 $^{\circ}$ C, and 30 s at 72 $^{\circ}$ C.

265 Amplified products were purified using the PureLink PCR Purification Kit (Thermo Fisher,  
266 K310002) and were sent for sequencing to Eurofins Genomics.

267

268 **Statistical analysis.** Data were analyzed with GraphPad Prism version 8. Confidence  
269 intervals were calculated using the modified Wald method. The Pearson correlation coefficient  
270 was used to assess the concordance between PCR  $C_T$  values.  $P$  values  $< 0.05$  were deemed  
271 significant.

272

## 273 **RESULTS**

274 **FEVER Computational Tool.** FEVER combines probes and primers generated to 1)  
275 broadly identify an entire class of virus; 2) specifically detect a strain of interest; and 3) detect  
276 SNPs of importance to public health. The computational approach starts with a curated multiple  
277 sequence alignment. The FEVER algorithm does not however require sequences to be aligned in  
278 order to generate assays. The alignment was performed to avoid overrepresentation of any single  
279 isolate and ensure broad coverage of the pathogen of interest. In March of 2020, we developed two  
280 alignments using the sequences available in GISAID: one with SARS-CoV-2 sequences and one  
281 with *Sarbecovirus* sequences. Of note our FEVER assays were developed within one month of the  
282 U.S. CDC assays (41) and also used viral sequence information obtained from GenBank. Next,  
283 our FEVER algorithm was applied to design probes using the *Sarbecovirus* alignment for  
284 biosurveillance and the SARS-CoV-2 alignment for diagnostics while also screening the results  
285 using parameters set for GC-content, hairpin propensity, and match recall to achieve high coverage  
286 as well as reagent manufacturing and performance compatibility. The FEVER algorithm identifies  
287 sets of probes that cover 100% of each multiple sequence alignment. Two pan-*Sarbecoviruses*

288 (FEVER\_5'UTR and FEVER\_Env) and two SARS-CoV-2 (FEVER\_ORF1ab and FEVER\_Spike)  
289 specific probes were needed to detect all input sequences. After the FEVER probes were designed,  
290 primers flanking the probe sites were designed using the PrimerDesign-M tool (44, 45) for use in  
291 RT-PCR assays (Table 1). Few variants were visually detected in the region of amplification of  
292 these primers and probes (Fig. S1). Further, we designed TaqMan SNP Genotyping PCR probes  
293 and primers to detect the previously identified A23403G (D614G amino acid change) mutation in  
294 the spike gene (40) (Table 1). Mutations in the SARS-CoV-2 genome conferring a fitness  
295 advantage have been reported (40). However, rapid methods to characterize SARS-CoV-2  
296 mutations are lacking. Together, the primers and probes for all three components (biosurveillance,  
297 diagnostics, and mutation typing) are referred to collectively as the FEVER assays.

298

299 ***In silico* inclusivity test.** We evaluated our FEVER assays using a public web-based  
300 validation tool against 525,708 sequences of SARS-CoV-2 (46). The *in silico* evaluation only  
301 included complete SARS-CoV-2 genome sequences that were at least 29 kb long. In general, a  
302 low number of predicted failures (false-negatives) was observed in comparison with the number  
303 of successes or true-positives (total of perfect matches, single mismatch, and double mismatches)  
304 (Table 2). Recall (true positives divided by the sum of true positives and false negatives) was used  
305 to assess relative assay performance. Of the FEVER and U.S. CDC assays, the SARS-CoV-2  
306 specific FEVER probe targeting ORF1ab had the best-predicted performance with a recall of  
307 99.7%. The pan-*Sarbecovirus* probe targeting the 5' UTR and envelope gene were also predicted  
308 to be highly inclusive for SARS-CoV-2 with recalls of 96.4% and 98.6%, respectively. In contrast,  
309 the SARS-CoV-2 specific probe targeting the spike gene had a 90.5% recall, suggesting that the  
310 spike gene is a suboptimal target due to its high genetic variability (40, 49). For instance, the U.S.

311 CDC N1 assay had a recall of 99.0% and the U.S. CDC N2 assay had a 99.2% recall. Compared  
312 with the U.S. CDC assays, the FEVER\_ORF1ab assay had a ~1% higher recall, FEVER\_Env had  
313 a similar recall, and the FEVER\_5'UTR and FEVER\_Spike assays had lower recall values.

314

315 **Analytical specificity.** Cross-reactivity of primers and probes with other microorganisms  
316 can reduce the efficacy of RT-PCR (50). For analysis of specificity, SARS-CoV-2 was the only  
317 target virus for the SARS-CoV-2 specific assays, and all sarbecoviruses were considered the  
318 targets for the pan-*Sarbecovirus* probes. We initially evaluated cross-reactivity *in silico* and then  
319 experimentally with non-target viruses. The specificity of each primer and probe set was tested *in*  
320 *silico* using BLAST, which yielded matches to SARS-CoV-2 only for the assay oligonucleotides  
321 specific to SARS-CoV-2 (FEVER\_ORF1ab and FEVER\_Spike) and matches to sarbecoviruses  
322 for the pan-*Sarbecovirus* assay oligonucleotides (FEVER\_5'UTR and FEVER\_Env). No hits to  
323 human DNA or other respiratory viruses were found.

324 For experimental evaluation of specificity, the FEVER assays were tested against three  
325 animal coronavirus strains (alphacoronavirus 1 strain Purdue P115, avian coronavirus strain  
326 Massachusetts, and porcine respiratory coronavirus strain ISU-1), four influenza virus strains  
327 (A/Brisbane/59/2007, A/Brisbane/10/2007, B/Nevada/03/2011, and B/Texas/06/2011), and a  
328 single strain of SARS-CoV (Urbani, isolated in 2003). The SARS-CoV-2 strain USA-WA1/2020  
329 was used as a positive control. The three animal coronavirus and four influenza virus strains all  
330 tested negative (Table 3). Excluding SARS-CoV-2, the SARS-CoV Urbani strain was the only  
331 commercially available genomic RNA from a *Sarbecovirus* available at the time of testing. The  
332 SARS-CoV Urbani strain was correctly tested negative by the U.S. CDC assays (N1 and N2),  
333 FEVER\_ORF1ab, and FEVER\_Spike targets. The SARS-CoV strain Urbani tested positive by the



334 pan-*Sarbecovirus* (FEVER\_5'UTR and FEVER\_Env) FEVER assays, which was expected  
 335 because these were designed to detect all sarbecoviruses. The SARS-CoV-2 strain USA-  
 336 WA1/2020 used as a positive control was correctly identified by both FEVER and U.S. CDC  
 337 assays.

**Table 3. Analytical specificity of the FEVER and U.S. CDC assays.**

Virus	Strain	GenBank Acc. # or Taxon ID <sup>a</sup>	FEVER				U.S. CDC	
			FEVER_5'UTR	FEVER_Env	FEVER_ORF1ab	FEVER_Spike	N1	N2
Alphacoronavirus 1	Purdue P115	DQ811788	-	-	-	-	-	-
Avian coronavirus	Massachusetts	GQ504724	-	-	-	-	-	-
Influenza A H1N1	A/Brisbane/59/2007	504904	-	-	-	-	-	-
Influenza A H3N2	A/Brisbane/10/2007	476294	-	-	-	-	-	-
Influenza B Victoria lineage	B/Nevada/03/2011	1308200	-	-	-	-	-	-
Influenza B Yamagata lineage	B/Texas/06/2011	1308263	-	-	-	-	-	-
Porcine respiratory coronavirus	ISU-1	DQ811787	-	-	-	-	-	-
SARS-CoV	Urbani	AY278741	+	+	-	-	-	-
SARS-CoV-2	USA-WA1/2020	MN985325	+	+	+	+	+	+

Abbreviations: +, detected; -, not detected.

<sup>a</sup>NCBI Taxon IDs were listed for influenza strains, which did not have a GenBank accession number.

338  
 339 **Analytical sensitivity in a NP swab matrix.** The analytical sensitivity and reproducibility  
 340 of each assay was tested using standard curves generated by three biological replicates of 10-fold  
 341 serial dilutions of SARS-CoV-2 spiked into human NP swab samples. The standard curves for RT-  
 342 PCR in NP swab samples had correlation coefficients (efficiency values) of 0.98 (100.9%) for  
 343 FEVER\_5'UTR, 0.99 (93.7%) for FEVER\_Env, 0.99 (96.5%) for FEVER\_ORF1ab, 0.99 (98.0%)  
 344 for FEVER\_Spike, 0.99 (103.2%) for N1, and 0.99 (99.1%) for N2, respectively (Fig. 1). We  
 345 demonstrated that both FEVER and U.S. CDC assays reliably detected SARS-CoV-2 at 1 copy/ $\mu$ L  
 346 spiked into an NP swab sample matrix.

347  
 348 **Comparison of FEVER and U.S. CDC RT-PCR results for clinical NP swab samples.**  
 349 Nasopharyngeal (NP) swab sampling is the recommended sampling method by the World Health  
 350 Organization (51) for nucleic acid amplification testing of SARS-CoV-2. Viral titers measured in  
 351 NP swabs vary depending on several factors, including disease progression (52-54). However, NP

352 swabs currently remain the reference sample type and support sensitive detection of SARS-CoV-  
 353 2 (55). Nasopharyngeal swabs from 100 COVID-19 patients were collected in New Mexico, U.S.  
 354 All assays were run under the same thermocycling conditions as per the U.S. CDC protocol (26).  
 355 All samples tested positive for the human RNase P gene used as a control to ensure success of the  
 356 RNA extraction and associated sample collection methods (Table S1). Of the 100 NP swab samples,  
 357 66% (66/100) were considered positive according to the U.S. CDC assays and testing criteria (37),  
 358 22 were negative and 12 samples yielded inconclusive results (Table 4). Samples that initially  
 359 produced an inconclusive result were re-tested and the 12 that remained inconclusive following  
 360 the second test were removed from the analysis of agreement, sensitivity, and specificity. We  
 361 compared the four FEVER assays to the results obtained with the U.S. CDC assays and found that  
 362 all four FEVER assays displayed 100% specificity (no false positives were detected) and varying  
 363 sensitivities ranging from 74.2% to 92.4% (Table 4, Table S1). However, the U.S. CDC assays  
 364 were performed in a Clinical Laboratory Improvement Amendments (CLIA)-certified laboratory,  
 365 while the FEVER assay was performed in a separate facility on a different thermocycler for  
 366 research purposes only.

**Table 4. FEVER assays compared to the U.S. CDC assays for detection of SARS-CoV-2 in 100 human patient nasopharyngeal swab samples.**

Result <sup>a</sup>	FEVER 5'UTR	FEVER Env	FEVER ORF1ab	FEVER Spike
Positive	61	56	56	49
Negative	39	44	44	51
Agreement <sup>b</sup>	94.3% (87.1-97.9%)	87.5% (78.8-93.0%)	88.6% (80.2-93.9%)	80.7% (71.1-87.7%)
Sensitivity <sup>c</sup>	92.4% (83.1-97.1%)	83.3% (72.4-90.6%)	84.8% (74.1-91.8%)	74.2% (62.5-83.3%)
Specificity <sup>d</sup>	100% (84.6-100%)	100% (84.6-100%)	100% (84.6-100%)	100% (84.6-100%)

<sup>a</sup> True values are as measured by the U.S. CDC assay criteria (37): 66 positive, 22 negative and 12 inconclusive. Samples initially recorded as inconclusive were re-tested and the 12 that remained inconclusive were removed from the analysis of agreement, sensitivity, and specificity.

<sup>b</sup>Agreement = no. of samples with identical results for an individual FEVER assay and U.S. CDC assay / 88

<sup>c</sup>Sensitivity = true positive / (true positive + false negative) with 95% confidence intervals

<sup>d</sup>Specificity = true negative / (true negative + false positive) with 95% confidence intervals

95% confidence intervals were calculated using the modified Wald method.

N/A, not applicable.

367

368 To directly compare the performance of the FEVER and U.S. CDC assays, 10 samples that  
369 contained sufficient remaining RNA were analyzed using both groups of assays on the same ABI  
370 StepOnePlus thermocycler in the same laboratory to avoid inter-instrument and inter-laboratory  
371 variability. The  $C_T$  values of the FEVER assays were plotted against those from the U.S. CDC  
372 assay (Fig. 2). In general, a broad range of  $C_T$  values from 13 to 39 was observed. Interestingly,  
373 one sample that originally tested positive for the U.S. CDC assay (N2) with a  $C_T$  value of 34 on  
374 the ABI 7500 Fast Dx, tested negative on the ABI StepOnePlus. There was a significant ( $P <$   
375 0.001), correlation between the  $C_T$  values of all four FEVER assays compared with each of the  
376 U.S. CDC N1 and N2 assays indicating that when run on the same instrument the FEVER and U.S.  
377 CDC assays yield highly similar  $C_T$  values (Fig. 2). It is unfortunate that this finding occurred after  
378 most of the patient samples were exhausted and so not all could be re-tested using the same  
379 instrument. These results highlight the importance of using the same instrument when comparing  
380  $C_T$  values for assay validation.

381  
382 **D614G mutation typing.** High-throughput tracking of SARS-CoV-2 mutations in patient  
383 samples may be essential for monitoring the spread of vaccine escape mutants (42). Sequencing  
384 can identify novel variants but is too expensive and time-consuming for high-throughput screening  
385 of patient samples to track the spread and movement of these variants on a global scale (40). To  
386 facilitate a rapid and high-throughput method for monitoring the spread of SNPs of interest, we  
387 have incorporated a SNP Genotyping PCR assay. For this mutation typing test, we are detecting  
388 the A23403G (D614G amino acid change) mutation in the spike gene, which is associated with  
389 greater infectivity (40) (Table 1). Control RNA from isolate USA-WA1/2020 (BEI Resources,  
390 NR-52347) was used as a positive control, and results showed that USA-WA1/2020 tested positive

391 for D614 (data not shown). Of the 59 SARS-CoV-2 positive patient samples (according to the  
392 FEVER assays), we determined the SNP at position 23,403 for 57 (96.6%) samples. The G23403  
393 variant was found in 57 samples and 2 samples were undetermined with a  $C_T$  cutoff of 45 (Table  
394 S2). A fragment of the spike gene was amplified, and the A23403G SNP was confirmed in a subset  
395 of samples (n=17) by sequencing (Table S3). These results indicate that most (57/59) patient  
396 isolates contained the mutated G614 form of SARS-CoV-2 that became prevalent globally in April  
397 2020 (40).

398

## 399 **DISCUSSION**

400 Early detection of emerging pathogens is required to mitigate outbreaks and prevent  
401 pandemics (10). Assays used for diagnosing infections are often used for biosurveillance; however,  
402 due to their high specificity, they are not usually suited for broad-spectrum surveillance  
403 applications or capable of identifying pathogen mutations (43, 56). Therefore, the user must often  
404 decide between either obtaining diagnostics or biosurveillance information but not both. FEVER  
405 (Fast Evaluation of Viral Emerging Risks) is a computational approach designed to simultaneously  
406 facilitate broad-spectrum biosurveillance, pathogen-specific diagnostics, and SNP variant tracking  
407 for pandemic response to any viral pathogen of interest. In this manuscript, we demonstrate the  
408 application of FEVER to the ongoing COVID-19 pandemic as an initial proof-of-concept. As a  
409 proof of concept, we present FEVER assays to detect all sarbecoviruses for future biosurveillance,  
410 SARS-CoV-2 for strain-specific diagnostics, and the D614G spike variant SNP mutation  
411 associated with increased transmissibility.

412 Here, we used an RT-PCR format to evaluate the performance of the FEVER assays as  
413 compared to the U.S. CDC assays. The success of RT-PCR as a diagnostic approach relies heavily

414 on the design quality of the primers and probes (57-59) as well as factors such as probe format,  
415 the ability to incorporate degenerate nucleotides, the number of target genomes that can be  
416 included in the design process to account for genetic diversity, and the ability to avoid cross-  
417 reactivity with near-neighbor genomes (60). In the case of SARS-CoV-2 diagnostics, it is also  
418 important that assays are able to differentiate infections caused by other common coronaviruses,  
419 in which case a false positive could result in unnecessary and costly mitigation procedures (61).  
420 For this reason, the U.S. CDC designed its N3 pan-*Sarbecovirus* assay; however, it was  
421 unfortunately removed from their assay in March of 2020 in order to expedite reagent  
422 manufacturing, consequently removing the biosurveillance component of the U.S. CDC COVID-  
423 19 assay (35, 37). This situation highlights the urgent need for a computational approach that can  
424 develop both biosurveillance and diagnostics assays that are screened for potential design issues  
425 that may potentially affect their performance and manufacturing.

426 Current probe design methods are also limited by over-representing single isolates in a  
427 sequence database as indicated by high coverage *in silico* but assay failure when novel variants  
428 emerge (31). In the case of SARS-CoV-2, the high number of false-negative results reported  
429 highlights the need for screening and updating assay designs as sequences become available (62-  
430 64), which has been a primary goal of <https://cov.lanl.gov>. Mutations in the probe or primer  
431 binding sites are particularly problematic since these can lead to false-negative results and  
432 infected individuals may continue to spread the disease (65). Pandemic preparedness requires a  
433 balanced approach combining targeted diagnostics assays designed to detect a specific outbreak  
434 strain with high-coverage biosurveillance assays that can account for pathogen mutation, and  
435 ideally this approach can be utilized to detect a variety of viral pathogens including those that are  
436 highly mutagenic. FEVER was designed to fill this void. In the case of SARS CoV-2, our assays

437 were developed within a month of the U.S. CDC assays also using publicly available sequence  
438 data, but with a different computational approach in mind. The U.S. CDC designed highly specific  
439 diagnostics assays by pre-selecting a single genomic target, the viral nucleocapsid gene, aligned a  
440 reference SARS-CoV-2 sequence (GenBank accession no. MN908947), and selected probe/primer  
441 sets with low similarity to other coronavirus sequences in GenBank (37). This method has yielded  
442 two SARS-CoV-2 specific assays that have contributed to combatting the current pandemic,  
443 however it is unclear how useful these assays will be in detecting the next coronavirus outbreak.

444 FEVER takes a more comprehensive approach to design robust multi-purpose assays to  
445 detect circulating viral strains and track their mutations but also to detect entire classes of viral  
446 pathogens in order to monitor emerging threats. The FEVER algorithm scans the entire viral  
447 genome to identify conserved regions and identifies the lowest possible number of probes  
448 necessary to cover all sequences scanned. The diagnostics probe FEVER\_ORF1ab displayed the  
449 highest coverage of SARS-CoV-2 sequences in this study with a predicted recall of 99.7%. It was  
450 predicted to detect all but 1,454 SARS-CoV-2 sequences out of 525,708 deposited in GISAID as  
451 of February 15, 2021. In comparison, the U.S. CDC N2 probe displayed 99.17% coverage and was  
452 predicted to fail in 4,353 sequences, which is nearly a 3-fold increase in false-negative results.

453 In addition to optimized sequence analysis, FEVER incorporates physical constraints set  
454 by the user to include GC-content, hairpin propensity, sequence length, and even mismatch  
455 tolerance. This ensures that probes selected for testing are thermodynamically compatible for  
456 increased assay performance as well as future multiplexing. It is critical that assay sensitivity is  
457 optimized as a 10-fold increase in the limit of detection for SARS-CoV-2 has shown to result in  
458 an increase in the false-negative rate by 13% (66). Here, the limit of detection for both the FEVER  
459 and U.S. CDC assays in NP swab samples was 1 copy/ $\mu$ L which matches previously published

460 findings (26). Additionally, FEVER assay design features can be used to ensure that probes and  
461 primers are suitable for large-scale manufacturing and can be tailored to a variety of biosensing  
462 platforms, including but not limited to RT-PCR. There is a clear need for the development of rapid  
463 and accurate point-of-care diagnostic tools to detect viral infections (67), and a variety of nucleic  
464 acid-based viral biosensors are in development for this purpose (43).

465 FEVER also includes a method for rapid mutation typing to track viral variants of public  
466 health importance. SARS-CoV-2 has proofreading mechanisms (68) and therefore relatively lower  
467 genetic diversity than other respiratory viruses such as influenza (69). For SARS-CoV-2, the  
468 predicted evolutionary rate is approximately  $8 \times 10^{-4}$  nucleotide substitution per site per year (69).  
469 The spike gene is under immune selective pressure as neutralizing antibodies against the protein  
470 product can inhibit viral entry into host cells (40, 70). SARS-CoV-2 acquired the D614G mutation  
471 in the spike protein early in the pandemic, and this mutation confers greater infectivity (71-73).  
472 Previously, the detection of this mutation has been based solely on viral sequencing, which is time-  
473 consuming and cost-prohibitive in many resource limited regions of the world (40, 61, 74, 75).  
474 FEVER incorporates a rapid PCR-based method for identifying the D614G mutation directly in  
475 patient samples. Similarly, mutation typing probes and primers can be designed in the future to  
476 track other variants of interest including the U.K. (B.1.1.7), South Africa (B.1.351), and Brazil  
477 (P.1) variants (41, 76, 77) to provide insight and real-time biosurveillance data on the circulation  
478 of potential vaccine escape variants.

479 In summary, the FEVER computational approach provides a novel tool to combat emerging  
480 viral pathogens. FEVER can be used for simultaneous biosurveillance of viruses, diagnostics of  
481 outbreak or pandemic isolates, and mutation typing to rapidly track the spread of variants  
482 impacting public health. In addition to PCR, FEVER can generate probes that are compatible with

483 a wide variety of nucleic acid sensing techniques which may be more suitable to point-of-care  
484 testing than RT-PCR (43). Here we show that the FEVER assays are comparable to those designed  
485 by the U.S. CDC for the detection of SARS-CoV-2 while simultaneously developing pan-  
486 *Sarbecovirus* assays for future biosurveillance applications. Additionally, FEVER mutation typing  
487 assays provide a rapid means for monitoring the spread of potential vaccine escape variants that  
488 may significantly impact a population. Future work will focus on applying FEVER towards the  
489 development of assays for the detection of other upper respiratory pathogens including influenza  
490 as well as testing FEVER probes in ultra-sensitive amplification-free nucleic acid biosensing  
491 platforms. FEVER provides a holistic computational approach to combine biosurveillance and  
492 diagnostics in order to better combat emerging viral pathogens.



## 493 SUPPORTING INFORMATION

494 **Figure S1. Visualization of SARS-CoV-2 variants in the amplified regions of FEVER and U.**  
495 **S. CDC RT-PCR assays.** Near-complete SARS-CoV-2 sequences (n = 299,404) were assessed  
496 from GISAID.org. The amplified regions of the FEVER assays (a) FEVER\_5'UTR, (b)  
497 FEVER\_Env, (c) FEVER\_ORF1ab, and (d) FEVER\_Spike and the U.S. CDC assays (e) N1 and  
498 (f) N2 were analyzed for SARS-CoV-2 variants. In each plot, no variants (N/A) were indicated by  
499 white and genomic positions containing variants were indicated by colored dots (green, blue,  
500 yellow or red). Plots were made using the Variant Visualizer that is under development and will  
501 be available at: <https://cov.lanl.gov>.

502

503 **Table S1. Raw  $C_T$  values of FEVER and U.S. CDC assays run on 100 human patient**  
504 **nasopharyngeal swab samples.**

505

506 **Table S2. Characterization of the D614G mutation among 59 SARS-CoV-2 positive patient**  
507 **nasopharyngeal swab samples.**

508

509 **Table S3. Sequence confirmation of the D614G mutation among 17 selected patient**  
510 **nasopharyngeal swab samples.**

511

## 512 ACKNOWLEDGMENTS

513 This research was funded by Los Alamos National Laboratory Exploratory Research and  
514 Development grant number 20190392ER (to J.K.S and K.Y.) and Los Alamos National Laboratory  
515 Technology Evaluation and Demonstration Funds. The authors would like to thank the

516 Presbyterian Clinical Research team (Brigitte Holder, Susan Salazar, and Maria Vahtel) for their  
517 contributions to this study. We are also grateful to the patients who volunteered to take part in this  
518 study.

519

## 520 REFERENCES

- 521 1. Reperant LA, Osterhaus A. 2017. AIDS, Avian flu, SARS, MERS, Ebola, Zika... what next?  
522 Vaccine 35:4470-4474.
- 523 2. Thompson WW, Shay DK, Weintraub E, Brammer L, Bridges CB, Cox NJ, Fukuda K. 2004.  
524 Influenza-associated hospitalizations in the United States. JAMA 292:1333-40.
- 525 3. Feldmann H. 2014. Ebola--a growing threat? N Engl J Med 371:1375-8.
- 526 4. Delisle E, Rousseau C, Broche B, Leparc-Goffart I, L'Ambert G, Cochet A, Prat C, Foulongne  
527 V, Ferre JB, Catelinois O, Flusin O, Tchernonog E, Moussion IE, Wiegandt A, Septfons A,  
528 Mendy A, Moyano MB, Laporte L, Maurel J, Jourdain F, Reynes J, Paty MC, Golliot F. 2015.  
529 Chikungunya outbreak in Montpellier, France, September to October 2014. Euro Surveill 20.
- 530 5. Ai J-W, Zhang Y, Zhang W. 2016. Zika virus outbreak: 'a perfect storm'. Emerging microbes  
531 & infections 5:e21-e21.
- 532 6. LeDuc JW, Barry MA. 2004. SARS, the First Pandemic of the 21st Century. Emerging  
533 Infectious Diseases 10:e26-e26.
- 534 7. Carrasco-Hernandez R, Jácome R, López Vidal Y, Ponce de León S. 2017. Are RNA Viruses  
535 Candidate Agents for the Next Global Pandemic? A Review. ILAR Journal 58:343-358.
- 536 8. Morens DM, Fauci AS. 2020. Emerging Pandemic Diseases: How We Got to COVID-19. Cell  
537 182:1077-1092.

- 538 9. Stromberg ZR, Fischer W, Bradfute SB, Kubicek-Sutherland JZ, Hrabec P. 2020. Vaccine  
539 Advances against Venezuelan, Eastern, and Western Equine Encephalitis Viruses. *Vaccines* 8.
- 540 10. Madhav N, Oppenheim B, Gallivan M, Mulembakani P, Rubin E, Wolfe N. 2017. Pandemics:  
541 Risks, Impacts, and Mitigation. *In* Jamison DT, Gelband H, Horton S, Jha P, Laxminarayan R,  
542 Mock CN, Nugent R (ed), *Disease Control Priorities: Improving Health and Reducing Poverty*  
543 doi:10.1596/978-1-4648-0527-1\_ch17, Washington (DC).
- 544 11. Carroll D, Morzaria S, Briand S, Johnson CK, Morens D, Sumption K, Tomori O,  
545 Wacharphaueasadee S. 2021. Preventing the next pandemic: the power of a global viral  
546 surveillance network. *BMJ* 372:n485.
- 547 12. Ibrahim NK. 2020. Epidemiologic surveillance for controlling Covid-19 pandemic: types,  
548 challenges and implications. *Journal of Infection and Public Health* 13:1630-1638.
- 549 13. Kobres P-Y, Chretien J-P, Johansson MA, Morgan JJ, Whung P-Y, Mukundan H, Del Valle  
550 SY, Forshey BM, Quandelacy TM, Biggerstaff M, Viboud C, Pollett S. 2019. A systematic  
551 review and evaluation of Zika virus forecasting and prediction research during a public health  
552 emergency of international concern. *PLOS Neglected Tropical Diseases* 13:e0007451.
- 553 14. Perkins MD, Dye C, Balasegaram M, Bréchet C, Mombouli JV, Røttingen JA, Tanner M,  
554 Boehme CC. 2017. Diagnostic preparedness for infectious disease outbreaks. *Lancet*  
555 390:2211-2214.
- 556 15. Manore C, Graham T, Carr A, Feryn A, Jakhar S, Mukundan H, Highlander HC. 2019.  
557 Modeling and Cost Benefit Analysis to Guide Deployment of POC Diagnostics for Non-  
558 typhoidal Salmonella Infections with Antimicrobial Resistance. *Scientific Reports* 9:11245.
- 559 16. Del Valle SY, McMahon BH, Asher J, Hatchett R, Lega JC, Brown HE, Leany ME, Pantazis  
560 Y, Roberts DJ, Moore S, Peterson AT, Escobar LE, Qiao H, Hengartner NW, Mukundan H.

- 561 2018. Summary results of the 2014-2015 DARPA Chikungunya challenge. *BMC Infectious*  
562 *Diseases* 18:245.
- 563 17. Kelly-Cirino CD, Nkengasong J, Kettler H, Tongio I, Gay-Andrieu F, Escadafal C, Piot P,  
564 Peeling RW, Gadde R, Boehme C. 2019. Importance of diagnostics in epidemic and pandemic  
565 preparedness. *BMJ global health* 4:e001179.
- 566 18. de Wilde AH, Snijder EJ, Kikkert M, van Hemert MJ. 2018. Host Factors in Coronavirus  
567 Replication. *Curr Top Microbiol Immunol* 419:1-42.
- 568 19. Paules CI, Marston HD, Fauci AS. 2020. Coronavirus Infections-More Than Just the Common  
569 Cold. *JAMA* 323:707-708.
- 570 20. Cui J, Li F, Shi Z-L. 2019. Origin and evolution of pathogenic coronaviruses. *Nature Reviews*  
571 *Microbiology* 17:181-192.
- 572 21. Wu F, Zhao S, Yu B, Chen Y-M, Wang W, Song Z-G, Hu Y, Tao Z-W, Tian J-H, Pei Y-Y,  
573 Yuan M-L, Zhang Y-L, Dai F-H, Liu Y, Wang Q-M, Zheng J-J, Xu L, Holmes EC, Zhang Y-  
574 Z. 2020. A new coronavirus associated with human respiratory disease in China. *Nature*  
575 579:265-269.
- 576 22. Zhu N, Zhang D, Wang W, Li X, Yang B, Song J, Zhao X, Huang B, Shi W, Lu R, Niu P,  
577 Zhan F, Ma X, Wang D, Xu W, Wu G, Gao GF, Tan W. 2020. A Novel Coronavirus from  
578 Patients with Pneumonia in China, 2019. *N Engl J Med* 382:727-733.
- 579 23. Sharma A, Tiwari S, Deb MK, Marty JL. 2020. Severe acute respiratory syndrome  
580 coronavirus-2 (SARS-CoV-2): a global pandemic and treatment strategies. *International*  
581 *Journal of Antimicrobial Agents* 56:106054-106054.

- 582 24. Fahmi M, Kubota Y, Ito M. 2020. Nonstructural proteins NS7b and NS8 are likely to be  
583 phylogenetically associated with evolution of 2019-nCoV. *Infection, Genetics and Evolution*  
584 81:104272.
- 585 25. Green DA, Zucker J, Westblade LF, Whittier S, Rennert H, Velu P, Craney A, Cushing M, Liu  
586 D, Sobieszczyk ME, Boehme AK, Sepulveda JL. 2020. Clinical Performance of SARS-CoV-  
587 2 Molecular Tests. *J Clin Microbiol* 58.
- 588 26. Centers for Disease Control and Prevention (CDC). 2020. CDC 2019-novel coronavirus  
589 (2019-nCoV) real-time RT-PCR diagnostic panel. [https://www.cdc.gov/coronavirus/2019-  
590 ncov/lab/rt-pcr-panel-primer-probes.html](https://www.cdc.gov/coronavirus/2019-ncov/lab/rt-pcr-panel-primer-probes.html). Accessed April 6, 2021.
- 591 27. Centers for Disease Control and Prevention (CDC). 2020. National institute for viral disease  
592 control and prevention. Specific primers and probes for detection of 2019 novel coronavirus.  
593 [http://ivdc.chinacdc.cn/kyjz/202001/t20200121\\_211337.html](http://ivdc.chinacdc.cn/kyjz/202001/t20200121_211337.html). Accessed April 6, 2021.
- 594 28. Chu DKW, Pan Y, Cheng SMS, Hui KPY, Krishnan P, Liu Y, Ng DYM, Wan CKC, Yang P,  
595 Wang Q, Peiris M, Poon LLM. 2020. Molecular Diagnosis of a Novel Coronavirus (2019-  
596 nCoV) Causing an Outbreak of Pneumonia. *Clin Chem* 66:549-555.
- 597 29. Corman VM, Landt O, Kaiser M, Molenkamp R, Meijer A, Chu DK, Bleicker T, Brünink S,  
598 Schneider J, Schmidt ML, Mulders DG, Haagmans BL, van der Veer B, van den Brink S,  
599 Wijsman L, Goderski G, Romette J-L, Ellis J, Zambon M, Peiris M, Goossens H, Reusken C,  
600 Koopmans MP, Drosten C. 2020. Detection of 2019 novel coronavirus (2019-nCoV) by real-  
601 time RT-PCR. *Euro surveillance* 25:2000045.
- 602 30. van Kasteren PB, van der Veer B, van den Brink S, Wijsman L, de Jonge J, van den Brandt A,  
603 Molenkamp R, Reusken C, Meijer A. 2020. Comparison of seven commercial RT-PCR  
604 diagnostic kits for COVID-19. *J Clin Virol* 128:104412.

- 605 31. SantaLucia J, Jr., Sozhamannan S, Gans JD, Koehler JW, Soong R, Lin NJ, Xie G, Olson V,  
606 Roth K, Beck L. 2020. Appendix Q: Recommendations for Developing Molecular Assays for  
607 Microbial Pathogen Detection Using Modern In Silico Approaches. *Journal of AOAC*  
608 *INTERNATIONAL* 103:882-899.
- 609 32. Medina RA, Rojas M, Tuin A, Huff S, Ferres M, Martinez-Valdebenito C, Godoy P, García-  
610 Sastre A, Fofanov Y, SantaLucia J, Jr. 2011. Development and characterization of a highly  
611 specific and sensitive SYBR green reverse transcriptase PCR assay for detection of the 2009  
612 pandemic H1N1 influenza virus on the basis of sequence signatures. *J Clin Microbiol* 49:335-  
613 44.
- 614 33. Sozhamannan S, Holland MY, Hall AT, Negrón DA, Ivancich M, Koehler JW, Minogue TD,  
615 Campbell CE, Berger WJ, Christopher GW, Goodwin BG, Smith MA. 2015. Evaluation of  
616 Signature Erosion in Ebola Virus Due to Genomic Drift and Its Impact on the Performance of  
617 Diagnostic Assays. *Viruses* 7:3130-3154.
- 618 34. Fitch JP, Gardner SN, Kuczmarski TA, Kurtz S, Myers R, Ott LL, Slezak TR, Vitalis EA,  
619 Zemla AT, McCready PM. 2002. Rapid development of nucleic acid diagnostics. *Proceedings*  
620 *of the IEEE* 90:1708-1721.
- 621 35. Vogels CBF, Brito AF, Wyllie AL, Fauver JR, Ott IM, Kalinich CC, Petrone ME, Casanovas-  
622 Massana A, Catherine Muenker M, Moore AJ, Klein J, Lu P, Lu-Culligan A, Jiang X, Kim DJ,  
623 Kudo E, Mao T, Moriyama M, Oh JE, Park A, Silva J, Song E, Takahashi T, Taura M,  
624 Tokuyama M, Venkataraman A, Weizman O-E, Wong P, Yang Y, Cheemarla NR, White EB,  
625 Lapidus S, Earnest R, Geng B, Vijayakumar P, Odio C, Fournier J, Bermejo S, Farhadian S,  
626 Dela Cruz CS, Iwasaki A, Ko AI, Landry ML, Foxman EF, Grubaugh ND. 2020. Analytical

- 627 sensitivity and efficiency comparisons of SARS-CoV-2 RT-qPCR primer-probe sets. *Nature*  
628 *Microbiology* 5:1299-1305.
- 629 36. Artesi M, Bontems S, Göbbels P, Franckh M, Maes P, Boreux R, Meex C, Melin P, Hayette  
630 M-P, Bours V, Durkin K. 2020. A Recurrent Mutation at Position 26340 of SARS-CoV-2 Is  
631 Associated with Failure of the E Gene Quantitative Reverse Transcription-PCR Utilized in a  
632 Commercial Dual-Target Diagnostic Assay. *Journal of Clinical Microbiology* 58:e01598-20.
- 633 37. Lu X, Wang L, Sakthivel SK, Whitaker B, Murray J, Kamili S, Lynch B, Malapati L, Burke  
634 SA, Harcourt J, Tamin A, Thornburg NJ, Villanueva JM, Lindstrom S. 2020. US CDC Real-  
635 Time Reverse Transcription PCR Panel for Detection of Severe Acute Respiratory Syndrome  
636 Coronavirus 2. *Emerging Infectious Diseases* 26:1654-1665.
- 637 38. Babiker A, Myers CW, Hill CE, Guarner J. 2020. SARS-CoV-2 Testing: Trials and  
638 Tribulations. *American Journal of Clinical Pathology* 153:706-708.
- 639 39. Nalla AK, Casto AM, Huang MW, Perchetti GA, Sampoleo R, Shrestha L, Wei Y, Zhu H,  
640 Jerome KR, Greninger AL. 2020. Comparative Performance of SARS-CoV-2 Detection  
641 Assays Using Seven Different Primer-Probe Sets and One Assay Kit. *J Clin Microbiol* 58.
- 642 40. Korber B, Fischer WM, Gnanakaran S, Yoon H, Theiler J, Abfalterer W, Hengartner N, Giorgi  
643 EE, Bhattacharya T, Foley B, Hastie KM, Parker MD, Partridge DG, Evans CM, Freeman TM,  
644 de Silva TI, McDanal C, Perez LG, Tang H, Moon-Walker A, Whelan SP, LaBranche CC,  
645 Sapphire EO, Montefiori DC. 2020. Tracking Changes in SARS-CoV-2 Spike: Evidence that  
646 D614G Increases Infectivity of the COVID-19 Virus. *Cell* 182:812-827.e19.
- 647 41. Tang JW, Tambyah PA, Hui DS. 2020. Emergence of a new SARS-CoV-2 variant in the UK.  
648 *J Infect* 82:e27-e28.

- 649 42. Williams TC, Burgers WA. 2021. SARS-CoV-2 evolution and vaccines: cause for concern?  
650 *Lancet Respir Med* 9:333-335.
- 651 43. Courtney SJ, Stromberg ZR, Kubicek-Sutherland JZ. 2021. Nucleic Acid-Based Sensing  
652 Techniques for Diagnostics and Surveillance of Influenza. *Biosensors (Basel)* 11:47.
- 653 44. Yoon H, Leitner T. 2015. PrimerDesign-M: a multiple-alignment based multiple-primer design  
654 tool for walking across variable genomes. *Bioinformatics* 31:1472-1474.
- 655 45. Brodin J, Krishnamoorthy M, Athreya G, Fischer W, Hrabec P, Gleasner C, Green L, Korber  
656 B, Leitner T. 2013. A multiple-alignment based primer design algorithm for genetically highly  
657 variable DNA targets. *BMC Bioinformatics* 14:255.
- 658 46. Li P-E, Myers y Gutiérrez A, Davenport K, Flynn M, Hu B, Lo C-C, Player Jackson E, Shakya  
659 M, Xu Y, Gans JD, Chain PSG. 2020. A public website for the automated assessment and  
660 validation of SARS-CoV-2 diagnostic PCR assays. *Bioinformatics*  
661 doi:10.1093/bioinformatics/btaa710.
- 662 47. Shu Y, McCauley J. 2017. GISAID: Global initiative on sharing all influenza data - from vision  
663 to reality. *Euro surveillance* 22:30494.
- 664 48. Li B, Kadura I, Fu DJ, Watson DE. 2004. Genotyping with TaqMAMA. *Genomics* 83:311-  
665 320.
- 666 49. Peñarrubia L, Ruiz M, Porco R, Rao SN, Juanola-Falgarona M, Manissero D, López-Fontanals  
667 M, Pareja J. 2020. Multiple assays in a real-time RT-PCR SARS-CoV-2 panel can mitigate the  
668 risk of loss of sensitivity by new genomic variants during the COVID-19 outbreak. *Int J Infect*  
669 *Dis* 97:225-229.



- 670 50. Qian J, Boswell SA, Chidley C, Lu Z-x, Pettit ME, Gaudio BL, Fajnzylber JM, Ingram RT,  
671 Ward RH, Li JZ. 2020. An enhanced isothermal amplification assay for viral detection. *Nature*  
672 *Communications* 11:5920.
- 673 51. World Health Organization. 2020. Laboratory testing for 2019 novel coronavirus (2019-  
674 nCoV) in suspected human cases, Interim guidance, 2 March 2020.  
675 <https://www.who.int/publications/i/item/10665-331501>. Accessed 05/11/2021.
- 676 52. Jamal AJ, Mozafarihashjin M, Coomes E, Powis J, Li AX, Paterson A, Anceva-Sami S, Barati  
677 S, Crowl G, Faheem A, Farooqi L, Khan S, Prost K, Poutanen S, Taylor M, Yip L, Zhong XZ,  
678 McGeer AJ, Mubareka S. 2021. Sensitivity of Nasopharyngeal Swabs and Saliva for the  
679 Detection of Severe Acute Respiratory Syndrome Coronavirus 2. *Clin Infect Dis* 72:1064-  
680 1066.
- 681 53. Wyllie AL, Fournier J, Casanovas-Massana A, Campbell M, Tokuyama M, Vijayakumar P,  
682 Warren JL, Geng B, Muenker MC, Moore AJ, Vogels CBF, Petrone ME, Ott IM, Lu P,  
683 Venkataraman A, Lu-Culligan A, Klein J, Earnest R, Simonov M, Datta R, Handoko R,  
684 Naushad N, Sewanan LR, Valdez J, White EB, Lapidus S, Kalinich CC, Jiang X, Kim DJ,  
685 Kudo E, Linehan M, Mao T, Moriyama M, Oh JE, Park A, Silva J, Song E, Takahashi T, Taura  
686 M, Weizman OE, Wong P, Yang Y, Bermejo S, Odio CD, Omer SB, Dela Cruz CS, Farhadian  
687 S, Martinello RA, Iwasaki A, Grubaugh ND, et al. 2020. Saliva or Nasopharyngeal Swab  
688 Specimens for Detection of SARS-CoV-2. *N Engl J Med* 383:1283-1286.
- 689 54. Klausner JD, Kojima N, Butler-Wu SM. 2021. Is the Patient Infected with SARS-CoV-2?  
690 *Journal of Clinical Microbiology* 59:e00147-21.

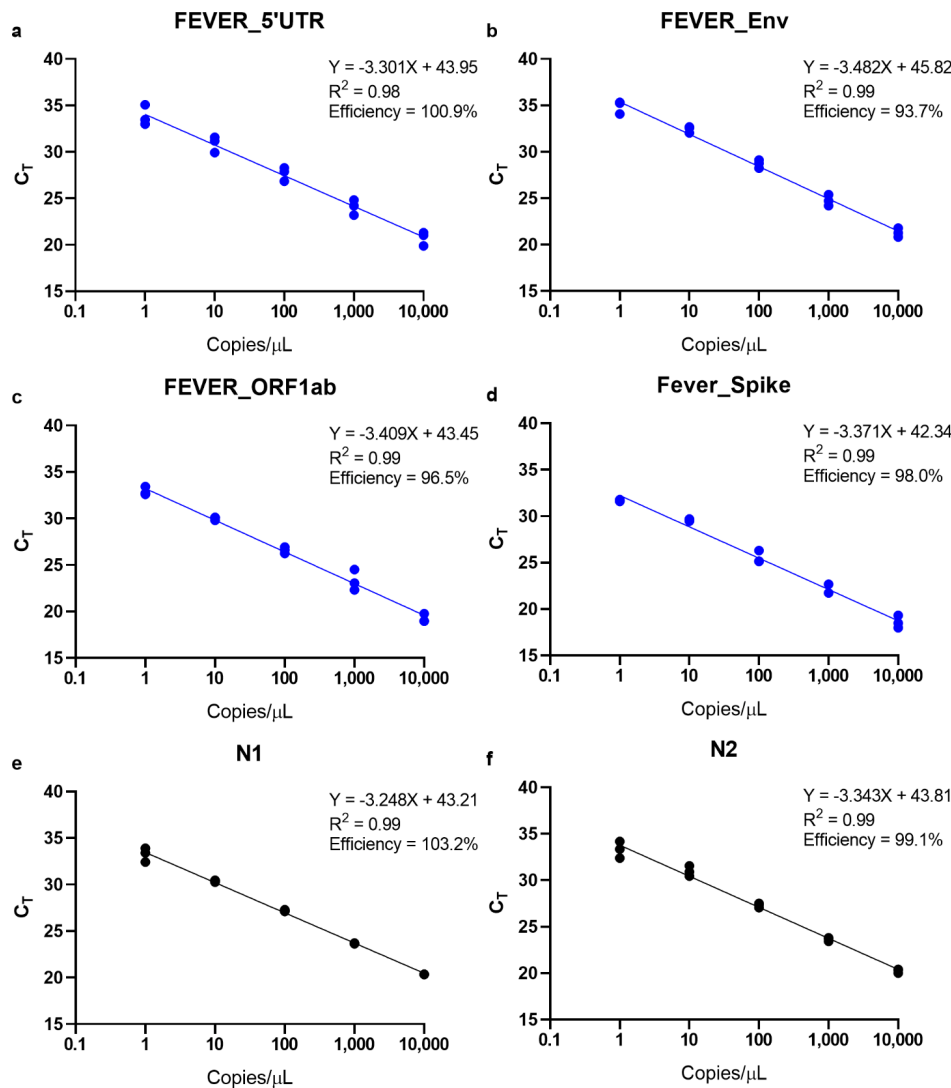
- 691 55. Bastos ML, Perlman-Arrow S, Menzies D, Campbell JR. 2021. The Sensitivity and Costs of  
692 Testing for SARS-CoV-2 Infection With Saliva Versus Nasopharyngeal Swabs : A Systematic  
693 Review and Meta-analysis. *Ann Intern Med* 174:501-510.
- 694 56. Hammou RA, Benhassou M, Bessi H, Ennaji MM. 2020. Chapter 7 - Scientific Advances in  
695 the Diagnosis of Emerging and Reemerging Viral Human Pathogens, p 93-120. *In* Ennaji MM  
696 (ed), *Emerging and Reemerging Viral Pathogens* doi:10.1016/B978-0-12-814966-9.00007-X.  
697 Academic Press.
- 698 57. Ye J, Coulouris G, Zaretskaya I, Cutcutache I, Rozen S, Madden TL. 2012. Primer-BLAST: a  
699 tool to design target-specific primers for polymerase chain reaction. *BMC Bioinformatics*  
700 13:134.
- 701 58. Hendling M, Pabinger S, Peters K, Wolff N, Conzemius R, Barišic I. 2018. Oli2go: an  
702 automated multiplex oligonucleotide design tool. *Nucleic Acids Res* 46:W252-W256.
- 703 59. Lopez-Rincon A, Tonda A, Mendoza-Maldonado L, Mulders DGJC, Molenkamp R, Perez-  
704 Romero CA, Claassen E, Garssen J, Kraneveld AD. 2021. Classification and specific primer  
705 design for accurate detection of SARS-CoV-2 using deep learning. *Scientific Reports* 11:947.
- 706 60. Li D, Zhang J, Li J. 2020. Primer design for quantitative real-time PCR for the emerging  
707 Coronavirus SARS-CoV-2. *Theranostics* 10:7150-7162.
- 708 61. Isabel S, Graña-Miraglia L, Gutierrez JM, Bundalovic-Torma C, Groves HE, Isabel MR,  
709 Eshaghi A, Patel SN, Gubbay JB, Poutanen T, Guttman DS, Poutanen SM. 2020. Evolutionary  
710 and structural analyses of SARS-CoV-2 D614G spike protein mutation now documented  
711 worldwide. *Scientific Reports* 10:14031.
- 712 62. Albert E, Ferrer B, Torres I, Serrano A, Alcaraz MJ, Buesa J, Solano C, Colomina J, Bueno F,  
713 Huntley D, Olea B, Valdivia A, Navarro D. 2021. Amplification of human  $\beta$ -glucuronidase

- 714 gene for appraising the accuracy of negative SARS-CoV-2 RT-PCR results in upper  
715 respiratory tract specimens. *J Med Virol* 93:48-50.
- 716 63. Gietema HA, Zelis N, Nobel JM, Lambriks LJG, van Alphen LB, Oude Lashof AML,  
717 Wildberger JE, Nelissen IC, Stassen PM. 2020. CT in relation to RT-PCR in diagnosing  
718 COVID-19 in The Netherlands: A prospective study. *PloS One* 15:e0235844-e0235844.
- 719 64. Richardson S, Hirsch JS, Narasimhan M, Crawford JM, McGinn T, Davidson KW, and the  
720 Northwell C-RC. 2020. Presenting Characteristics, Comorbidities, and Outcomes Among 5700  
721 Patients Hospitalized With COVID-19 in the New York City Area. *JAMA* 323:2052-2059.
- 722 65. Woloshin S, Patel N, Kesselheim AS. 2020. False Negative Tests for SARS-CoV-2 Infection  
723 - Challenges and Implications. *N Engl J Med* 383:e38.
- 724 66. Arnaout R, Lee RA, Lee GR, Callahan C, Cheng A, Yen CF, Smith KP, Arora R, Kirby JE.  
725 2021. The Limit of Detection Matters: The Case for Benchmarking Severe Acute Respiratory  
726 Syndrome Coronavirus 2 Testing. *Clin Infect Dis* doi:10.1093/cid/ciaa1382.
- 727 67. Ravi N, Cortade DL, Ng E, Wang SX. 2020. Diagnostics for SARS-CoV-2 detection: A  
728 comprehensive review of the FDA-EUA COVID-19 testing landscape. *Biosens Bioelectron*  
729 165:112454-112454.
- 730 68. Robson F, Khan KS, Le TK, Paris C, Demirbag S, Barfuss P, Rocchi P, Ng WL. 2020.  
731 Coronavirus RNA Proofreading: Molecular Basis and Therapeutic Targeting. *Mol Cell*  
732 79:710-727.
- 733 69. MacLean OA, Orton RJ, Singer JB, Robertson DL. 2020. No evidence for distinct types in the  
734 evolution of SARS-CoV-2. *Virus Evolution* 6.
- 735 70. Lo Presti A, Rezza G, Stefanelli P. 2020. Selective pressure on SARS-CoV-2 protein coding  
736 genes and glycosylation site prediction. *Heliyon* 6:e05001.

- 737 71. Weissman D, Alameh MG, de Silva T, Collini P, Hornsby H, Brown R, LaBranche CC,  
738 Edwards RJ, Sutherland L, Santra S, Mansouri K, Gobeil S, McDanal C, Pardi N, Hengartner  
739 N, Lin PJC, Tam Y, Shaw PA, Lewis MG, Boesler C, Şahin U, Acharya P, Haynes BF, Korber  
740 B, Montefiori DC. 2020. D614G Spike Mutation Increases SARS CoV-2 Susceptibility to  
741 Neutralization. *Cell Host Microbe* 29:23-31.e4.
- 742 72. Mansbach RA, Chakraborty S, Nguyen K, Montefiori DC, Korber B, Gnanakaran S. 2021. The  
743 SARS-CoV-2 Spike variant D614G favors an open conformational state. *Science Advances*  
744 7:eabf3671.
- 745 73. Plante JA, Liu Y, Liu J, Xia H, Johnson BA, Lokugamage KG, Zhang X, Muruato AE, Zou J,  
746 Fontes-Garfias CR, Mirchandani D, Scharton D, Bilello JP, Ku Z, An Z, Kalveram B, Freiberg  
747 AN, Menachery VD, Xie X, Plante KS, Weaver SC, Shi P-Y. 2020. Spike mutation D614G  
748 alters SARS-CoV-2 fitness. *Nature* 592:116-121.
- 749 74. Gong YN, Tsao KC, Hsiao MJ, Huang CG, Huang PN, Huang PW, Lee KM, Liu YC, Yang  
750 SL, Kuo RL, Chen KF, Liu YC, Huang SY, Huang HI, Liu MT, Yang JR, Chiu CH, Yang CT,  
751 Chen GW, Shih SR. 2020. SARS-CoV-2 genomic surveillance in Taiwan revealed novel  
752 ORF8-deletion mutant and clade possibly associated with infections in Middle East. *Emerg*  
753 *Microbes Infect* 9:1457-1466.
- 754 75. Slezak T, Kuczmarski T, Ott L, Torres C, Medeiros D, Smith J, Truitt B, Mulakken N, Lam  
755 M, Vitalis E, Zemla A, Zhou CE, Gardner S. 2003. Comparative genomics tools applied to  
756 bioterrorism defence. *Briefings in Bioinformatics* 4:133-149.
- 757 76. Tang JW, Toovey OTR, Harvey KN, Hui DDS. 2021. Introduction of the South African SARS-  
758 CoV-2 variant 501Y.V2 into the UK. *The Journal of infection* 82:e8-e10.

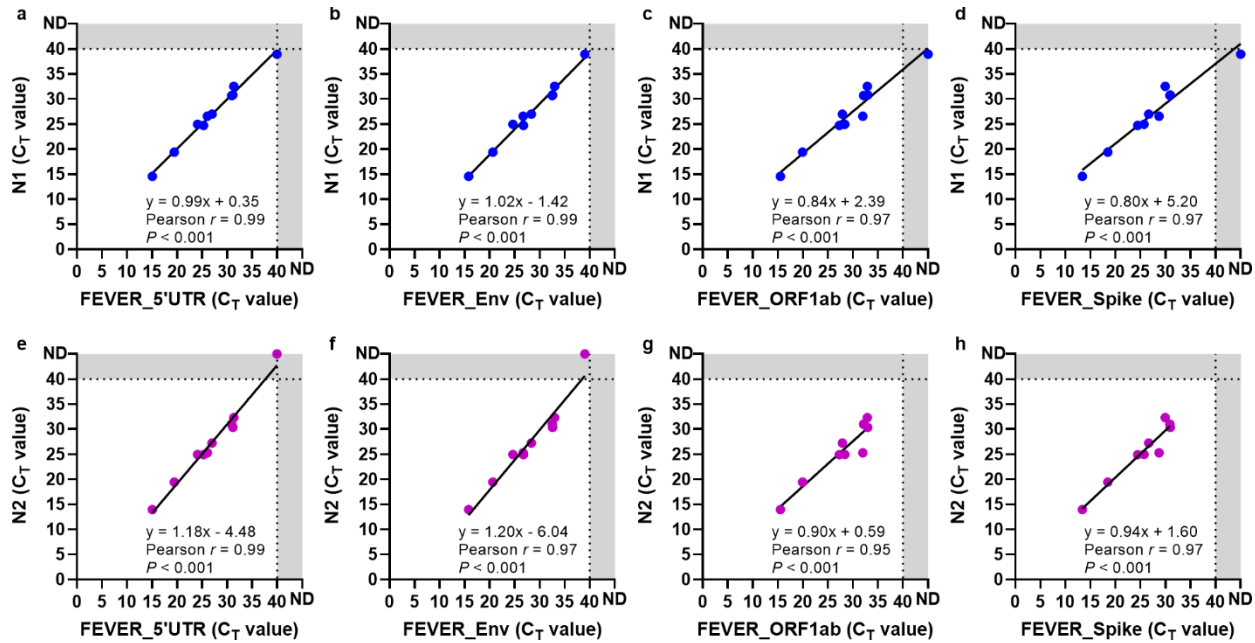
759 77. La Rosa G, Mancini P, Bonanno Ferraro G, Veneri C, Iaconelli M, Lucentini L, Bonadonna L,  
760 Brusaferrero S, Brandtner D, Fasanella A, Pace L, Parisi A, Galante D, Suffredini E. 2021. Rapid  
761 screening for SARS-CoV-2 variants of concern in clinical and environmental samples using  
762 nested RT-PCR assays targeting key mutations of the spike protein. *Water Res* 197:117104.

763 **FIGURES**



764

765 **Figure 1. FEVER assays can detect 1 copy/ $\mu$ L SARS-CoV-2 spiked into a nasopharyngeal**  
766 **swab sample matrix.** Inactivated SARS-CoV-2 strain USA-WA1/2020 was spiked into human  
767 nasopharyngeal swab samples (confirmed to be SARS-CoV-2 negative) and serial 10-fold diluted  
768 from  $10^4$  to 1 copies/ $\mu$ L. Cycle threshold ( $C_T$ ) values were determined for FEVER assays (blue  
769 dots) (a) FEVER\_5'UTR, (b) FEVER\_Env, (c) FEVER\_ORF1ab, and (d) FEVER\_Spike and the  
770 (a) N1 and (b) N2 assay described by the U.S. CDC (black dots).



771

772

773

774

775

776

777

778

779

**Figure 2. The FEVER and U.S. CDC assays show concordance in detecting SARS-CoV-2 in patient nasopharyngeal swab samples.** The U.S. CDC N1 cycle threshold (C<sub>T</sub>) values were compared to (a) FEVER\_5'UTR, (b) FEVER\_Env, (c) FEVER\_ORF1ab, and (d) FEVER\_Spike RT-PCR assays C<sub>T</sub> values (blue dots). The U.S. CDC N2 C<sub>T</sub> values were compared to (e) FEVER\_5'UTR, (f) FEVER\_Env, (g) FEVER\_ORF1ab, and (h) FEVER\_Spike RT-PCR assays C<sub>T</sub> values (purple dots). One sample was removed for the N2 vs FEVER\_ORF1ab and N2 vs FEVER\_Spike comparisons because it was not detected by these assays. Each dot represents an individual sample. Dotted lines represent the limit of detection. ND, not detected.